Neutron investigation of incommensurability and metastability in NH_4HSeO_4 and ND_4DSeO_4

F. Dénoyer, A. Rozycki, and K. Parlinski*
Laboratoire de Physique des Solides, Bâtiment 510, Université de Paris–Sud, 91405 Orsay, France

M. More†
Laboratoire Léon Brillouin, Centre d'Etudes Nucléaires de Saclay, 91191 Gif-sur-Yvette Cédex, France
(Received 9 May 1988)

This paper reports results of a neutron diffraction study on NH_4HSeO_4 and ND_4DSeO_4 single crystals. In NH_4HSeO_4 the measurements give direct evidence for an incommensurate phase existing between the high-temperature monoclinic phase (space group $B2$) and the low-temperature ferroelectric lock-in phase ($k=\frac{1}{3}$) (space group $P1$). Some of the high-temperature monoclinic, incommensurate, and ferroelectric phases are long-living metastable states. Room-temperature ND_4DSeO_4, being orthorhombic (space group $P2_12_12_1$), transforms at high temperatures into a stable incommensurate phase with the parent lattice of $B2$ symmetry. At even higher temperatures the monoclinic phase (space group $B2$) is restored. With decreasing temperature first the stable incommensurate phase, next a partly stable and partly metastable lock-in $k=\frac{1}{4}$ phase, and then a metastable long-living ferroelectric $k=\frac{1}{3}$ phase appears. At low temperatures, the orthorhombic phase $P2_12_12_1$ is stable. Evidence for the growth processes of the $P2_12_12_1$ phase within the lock-in $k=\frac{1}{4}$ phase is given. Between the lock-in phases $k=\frac{1}{4}$ and $\frac{1}{3}$, states with several coexisting modulations have been observed on cooling. A group-theoretical analysis of the incommensurate phases is also made.

I. INTRODUCTION

Ammonium hydrogen selenate crystals exhibit many interesting physical properties related to high ionic conductivity, incommensurability, and ferroelectricity. A considerable amount of information is already available in the literature. The phase diagram[1] is shown in Fig. 1. NH_4HSeO_4 has the following phase sequence:

$$\text{superionic} \xrightarrow{T_{SI}=417\text{ K}} \text{paraelectric} \xrightarrow{T_i=260\text{ K}} \text{intermediate} \xrightarrow{T_c=252\text{ K}} \text{ferroelectric} \xrightarrow{T_L=98\text{ K}} \text{low temperature},$$

however, the structure of the intermediate and paraelectric phases has been found "unstable."[1] The crystal structures in the paraelectric (293 K) (Ref. 2) and ferroelectric (223 K) (Ref. 3) phases have been determined by x-ray diffraction (Fig. 2). The structures of other phases have not been studied. In the paraelectric phase, NH_4HSeO_4 is monoclinic with space group $B2$ ($Z=6$, $a=19.745$ Å, $b=4.611$ Å, $c=7.552$ Å, $\gamma=102°35'$).[2] The ferroelectric phase results from a small distortion of the monoclinic $B2$ cell giving rise to a pseudomonoclinic "nonstandard space group $B1$" ($Z=6$, $a=19.593$ Å, $b=4.598$ Å, $c=7.507$ Å, $\alpha=90.02°$, $\beta=89.03°$, $\gamma=102.13°$).[3] Recently very weak superlattice reflections $(h,k,l\pm\frac{1}{3})$ were observed at $T=223$ K in the ferroelectric phase, demonstrating that the pseudomonoclinic unit cell is tripled along the **c** direction.[4]

Deuterated ammonium hydrogen selenate ND_4DSeO_4 crystallizes in the orthorhombic symmetry with space group $P2_12_12_1$ ($Z=4$, $a=12.887$ Å, $b=4.599$ Å, $c=7.515$ Å) (Refs. 5 and 6) [cf. Fig. 2(b)]. This phase is stable down to lowest temperature (about 10 K).[7] Partially deuterated crystals $(NH_4)_{1-x}(ND_4)_xH_{1-x}D_xSeO_4$ with $x>0.5$ crystallize in the same orthorhombic phase.[5] On heating, a polymorphic phase transition from the orthorhombic structure to the $B2$ structure occurs at T_P (Refs. 5 and 8) (for example, $T_P\sim330$ K for crystals with $x=0.6$). It was suggested[1,9] that after passing through T_P the crystals recover the phase sequence of pure NH_4HSeO_4 and partially deuterated crystals (with $x<0.5$) (cf. Fig. 1); however, recent x-ray diffraction experiments on ND_4DSeO_4 have revealed a situation rather more complicated.[4] In particular a $2c$ superstructure has been found at $T=310$ K in the intermediate phase. The temperature-range "stability" of this phase is not yet known. An open question remains whether the commensurate phase is preceded by the incommensurate one or not. Nothing is known about the phase transition from the $2c$ superstructure to the ferroelectric phase. Does an incommensurate phase exist between the $2c$-commensurate and the ferroelectric phase? Finally it has been recently pointed out that in ND_4DSeO_4 the structures of the intermediate and ferroelectric phases are also

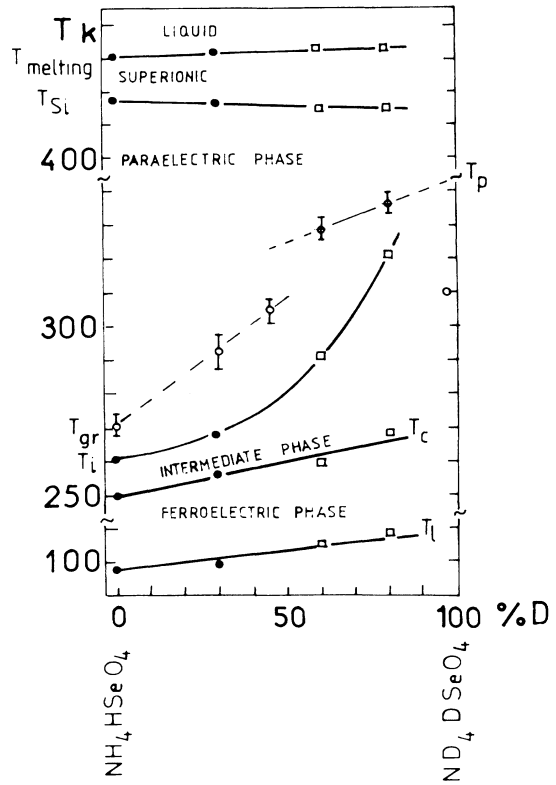

FIG. 1. Temperature, deuterium concentration phase diagram of $(NH_4)_{1-x}(ND_4)_xH_{1-x}D_xSeO_4$ from Refs. 1 and 10 ($x = \%D$).

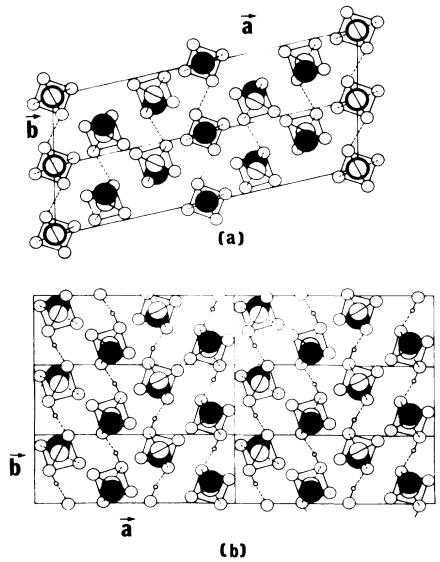

FIG. 2. Comparison between projections on the (**a**,**b**) plane of (a) the $B2$ monoclinic structure from Ref. 2 and (b) $P2_12_12_1$ orthorhombic structure from Ref. 6; solid circles represent NH_4, small circles H, medium circles O, and large circles Se; in the $B2$ monoclinic structure the protons are disordered in the O—H—O hydrogen bonds. Two monoclinic and six orthorhombic unit cells have been drawn in order to show the relationship between the two sets of crystallographic axes.

"unstable."[4] The accompanying nonequilibrium processes have been recently identified as corresponding to the growing of the orthorhombic $P2_12_12_1$ phase either in the paraelectric phase (NH_4HSeO_4) (Refs. 4 and 10) or in the intermediate and ferroelectric phases [NH_4HSeO_4 (Refs. 4 and 10), ND_4DSeO_4 (Ref. 4)]. For mixed $(NH_4)_{1-x}(ND_4)_xH_{1-x}D_xSeO_4$ crystals with $x < 0.5$, the growing of the $P2_12_12_1$ phase has been recently observed below the line $T_{gr}(x)$,[10] and this line has been drawn in Fig. 1.

After a preliminary x-ray diffraction experiment using a photography technique, which has allowed localization in reciprocal space of the structural features which are the signatures of the incommensurability and metastability,[4] we have decided to undertake more accurate quantitative counter measurements on NH_4HSeO_4 and ND_4DSeO_4. Neutron diffraction has been chosen because it is particularly well suited to study the modifications concerning the ordering of protons or deuterium in the different phases. Below we report results of these studies.

II. EXPERIMENTAL METHOD

NH_4HSeO_4 and ND_4DSeO_4 crystals were prepared by mixing an excess of H_2SeO_4 (or D_2SeO_4), 0.75M, with $(NH_4)_2SeO_4$ [or $(ND_4)_2SeO_4$]. Colorless and transparent single crystals were grown in aqueous solution by slow cooling from 327 to 317 K. Several months are necessary to obtain crystals of about 2 cm^3. One pure hydrogenated and one fully deuterated (% D > 95) single-crystal specimen were cut from these large samples; they had parallelepipedic shapes ($4\times8.6\times5.5$ mm^3 for NH_4HSeO_4 and $5.7\times8.6\times4$ mm^3 for ND_4DSeO_4) with faces perpendicular to the **a**+**b**, **b**, and **c** axes (relative to the monoclinic phase) or to the **a**, **b**, and **c** axes (relative to the orthorhombic phase); the specimens were placed, free of stresses, in aluminum cells, the cells being themselves located inside a variable-temperature cryostat. Since NH_4HSeO_4 and ND_4DSeO_4 are highly hygroscopic, manipulation of specimens was done in an atmosphere of dry nitrogen. Neutron diffraction experiments were performed on the three-axes spectrometer G 4-3, installed on a cold guide at the ORPHEE Reactor (Laboratoire Léon Brillouin, Saclay, France). The spectrometer was operated in the elastic mode using a Be-filtered incident neutron wavelength of 3.98 Å, collimations were adjusted to 30′-30′-30′.

Figure 3 shows the scattering plane and the relationship between the orthorhombic and monoclinic indexing when the polymorphic $B2 \rightarrow P2_12_12_1$ transformation occurs. All measurements were performed in the $(\bar{h}hl)$ zone (monoclinic notation); we concentrate mostly on (i) $(\bar{2}2\pm q)$ satellite reflections to study the problem of incommensurability, (ii) (002),($\bar{2}$20) Bragg reflections to detect the amount of the monoclinic $B2$ phase, and (iii) (021) Bragg reflection which is a measure of the amount of oriented grown $P2_12_12_1$ phase within the $B2$, intermediate, or $P1$ phases. Their positions, widths, and intensities were monitored as a function of temperature. A

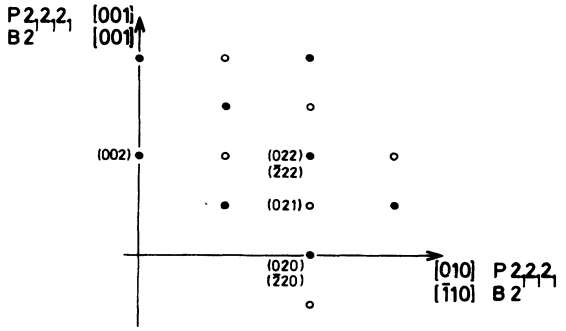

FIG. 3. Scattering plane and relationship between the orthorhombic and monoclinic indexing when the polymorphic $B2 \rightarrow P2_12_12_1$ transformation occurs. In the orthorhombic structure $(0kl)$ reflections obey extinction rules: (i) $k=0$ and $l=2n+1$ and (ii) $l=0$ and $k=2n+1$ (solid and open dots correspond to observable Bragg reflections). In the monoclinic structure $(\bar{h}hl)$ reflections verify extinction rules $h+l=2n+1$ (only solid dots). The terminology used in the text is as follows: when we discuss problems related to modulated phases, the parent lattice being monoclinic $B2$, we use the monoclinic indexing, but when we discuss nonequilibrium problems related to the nucleation and growth of the orthorhombic phase $P2_12_12_1$ we use the orthorhombic indexing.

systematic interplanar distances $d_{(\bar{1}10)}$ and $d_{(001)}$ calibration has been done for each temperature.

III. RESULTS

A. NH_4HSeO_4

Ammonium hydrogen selenate exists in two crystal structures: $P2_12_12_1$ orthorhombic and $B2$ monoclinic. It was reported in Refs. 1, 4, and 10 that below $T_{gr}=271$ K the orthorhombic phase is stable as is the paraelectric one above T_{gr}. However, below T_{gr} the polymorphic transformation from the metastable paraelectric or even intermediate phase to the stable orthorhombic one is very slow and the time of this transformation is found to vary between a few to a few tens of hours, depending on the sample quality, external stresses, and temperature cycling. The long time, therefore, allows study of the metastable phase. However, to complete the data we have summarized the thermal history of our sample in Fig. 4.

In the first cooling run (AB), in order to demonstrate that the intermediate phase is incommensurate, only a few data points were taken (cf. Fig. 4). A systematic check of satellite reflections has been made in scanning along the $\mathbf{c}^*$ direction in the $(\bar{h}hl)$ scattering plane for $h=0$, 1, and 2. Except in the (002) zone, satellite reflections were found, in between T_i and T_c, in any zone within the reach of 1.58-Å^{-1} incident neutrons, i.e., $(\bar{1}11)$, $(\bar{1}13)$, and $(\bar{2}20)$; the satellite wave vector $\mathbf{k}_z=k(004\pi/c)$ has been found to smoothly increase with decreasing temperature. At T_c it locks in discontinuously onto the rational value $k=\frac{1}{3}$ (Fig. 5). The width of satellite reflection remains in the limit of the resolution and no higher-order satellite reflections could be detected even near T_c. During this first cooling run,

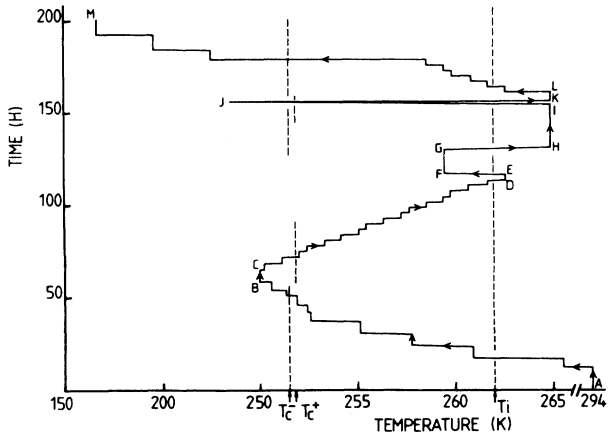

FIG. 4. Thermal history of the NH_4HSeO_4 sample.

no oriented growth of the $P2_12_12_1$ orthorhombic phase within the incommensurate or ferroelectric phases could be observed. If growth has occurred without relationship between the two sets of crystallographic axes, we would be unable to estimate this crystal volume which has been transformed into the orthorhombic phase. For these reasons, we are not sure that the variation of the order parameter as a function of temperature is correct, nevertheless, it seems worthwhile to show as a reference curve the variation of the satellite intensity during this first cooling run (cf. Fig. 6). At the lock-in temperature T_c only a small jump is observed. Therefore the growing of the $P2_12_12_1$ orthorhombic phase does not seem to be so drastic and surprisingly does not prevent the continuation of the experiment.

In order to obtain a more accurate determination of the modulation wave number as a function of temperature, in the subsequent heating run (CD) (cf. Fig. 4) data

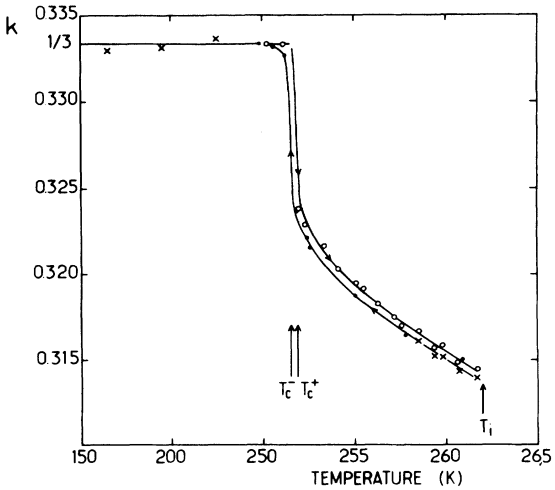

FIG. 5. Temperature dependence of the wave number $k(T)$ in NH_4HSeO_4, obtained during cooling run (AB) (●), heating run (CD) (○), and cooling run (LM) (×), as shown in Fig. 4. $T_i=262$ K, $T_c^-=251.5$ K, and $T_c^+=251.8$ K.

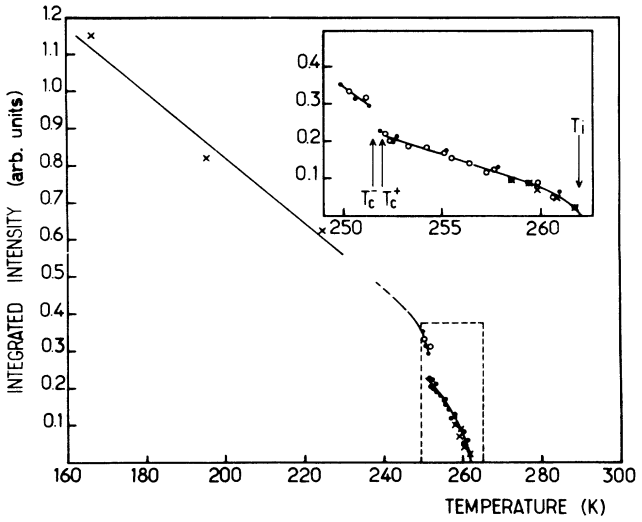

FIG. 6. Integrated intensity of the $(\bar{2}\,2\pm q)$ satellite reflections in NH_4HSeO_4 as a function of temperature (cf. Fig. 5 for the definition of symbols).

points have been taken at a regular rate of one point per 160 min with the temperature steps typically of the order of 1 K. Starting from the ferroelectric lock-in phase $k=\frac{1}{3}$, the modulation wave number jumps at T_c to $k\approx 0.324$, then smoothly decreases down to $k(T_i)$ ≈ 0.314 (Fig. 5). Lock-in transition at T_c is affected by a small temperature hysteresis of approximately 0.3 K and a global hysteresis of $k(T)$ is observed throughout the incommensurate phase. This type of behavior is a characteristic feature of many modulated structures. A comparison (Fig. 6) of the satellite intensity with the intensity obtained during the first cooling run shows that in the heating run (CD), the $P2_12_12_1$ orthorhombic phase does not grow inside the incommensurate phase. Probably, the time of neutron measurements was too short to allow for our sample a development of the $P2_12_12_1$ orthorhombic phase and *under these circumstances* the sequence of phase transitions, paraelectric, incommensurate, ferroelectric, is *reversible*. We suppose that below $T_{gr}\approx 271$ K, the transformation to the stable $P2_12_12_1$ orthorhombic phase needs a much longer time. Similar effects have been observed in cyanoadamantane.[11] To obtain more information on the transformation time, the temperature was kept constant for 13 and 24 h at 259.4 K (FG) and at 264.9 K (HI), respectively. At both temperatures no change of (002) and $(\bar{2}20)$ fundamental Bragg peaks of the monoclinic phase or $(\bar{2}2\pm q)$ satellite reflections of the incommensurate phase, or (021) Bragg reflection of the orthorhombic could be detected. The situation became slightly different after a temperature cycling between 264.9 and 237 K [path (IJK), cf. Fig. 4]. A comparison of the scans at the same temperature ($T=264.9$ K), just before and after cycling, revealed a 10% and 2% decrease of the (002) and $(\bar{2}20)$ Bragg reflections, respectively. Repeated scans during 5 h were unsuccessful in showing any evolution. No (021) Bragg reflection could be detected. Therefore, the possibility is excluded that the growth of the $P2_12_12_1$ orthorhombic phase within the $B2$ monoclinic-phase occurs with such a relationship between the two sets of crystallographic axes as mentioned in Fig. 3. However, the asymmetry in the reduction of the intensity between the (002) and $(\bar{2}20)$ reflections signifies that some grains have grown conserving one crystallographic axis. A comparison at $T=264.9$ K of the extrapolated intensities obtained during the first cooling run (AB) and intensities obtained during the path (HI) revealed reductions of $\sim 6\%$ and 9% for $(\bar{2}20)$ and (002) reflections, respectively. That allows us to conclude that the orthorhombic phase had started to grow. During the subsequent cooling run [path (LM), Fig. 4] we decided to complete the wave-vector variation in the incommensurate phase in the vicinity of T_i and to study the ferroelectric lock-in phase down to 166 K. Between the two cooling runs [paths (AB) and (LM)] a small amount of orthorhombic phase has already grown. For example, at $T=259.4$ K, the intensity reduction of $\sim 5\%$ and $\sim 16\%$ for $(\bar{2}20)$ and (002) Bragg reflection are observed. Indeed, the points in the second cooling run ($\times$) are systematically lower than in the first cooling run (●), cf. Fig. 6. These modifications do not seem to affect the temperature dependence of the wave number. The measurements below T_c of the ferroelectric lock-in phase $k=\frac{1}{3}$ are in agreement with the triclinic symmetry with space group $P1$ (see Sec. IV and Ref. 3) where the angle γ' between the $\mathbf{a}^*+\mathbf{b}^*$ and $\mathbf{c}^*$ directions does not remain equal to 90°. A splitting of the $(\bar{2}20)$ Bragg reflection into two peaks of equal intensity gives evidence for a twinned sample. This splitting leads to an angular separation Δ equal to 0.36° at $T=225$ K. It slightly increases with decreasing temperature and reaches, at $T=166.5$ K, $\Delta=0.40°$. The angle γ' is directly related to Δ by the following expression: $\gamma'=90°-\Delta/2$. Splitting of $(\bar{2}\,2\,\frac{2}{3})$ superstructure reflection into two components along the $\mathbf{c}^*$ direction was also observed. The splitting resulted from these two types of domains. In the measurements of the interplanar distances $d_{(001)}$ and $d_{(\bar{1}10)}$, a perfect temperature reproducibility was observed.

B. ND_4DSeO_4

Time is an important parameter in such compounds, and Fig. 7 reports the thermal history of our sample during the experiment.

1. First heating run: transformation from $P2_12_12_1$ to the incommensurate phase

Starting with a virgin sample in its original growing phase of $P2_12_12_1$ symmetry [(AB), Fig. 7] the single crystal has been warmed up to 342.7 K, in order to restore the phase sequence of Fig. 1. Scans along the $\mathbf{c}^*$ direction in the $(\bar{h}hl)$ reciprocal plane (monoclinic notation) reveal, at this temperature, (i) main Bragg reflection $(\bar{h}hl)$ obeying the extinction rule $h+l=2n+1$ compatible with the $B2$ structure and (ii) satellite diffraction peaks, situated at $(\bar{1}\,1\,0.5198)$, $(\bar{1}\,1\,1.4802)$, $(\bar{1}\,1\,2.5198)$, and $(\bar{2}\,2\pm 0.4802)$, i.e., in any zone accessible in this experi-

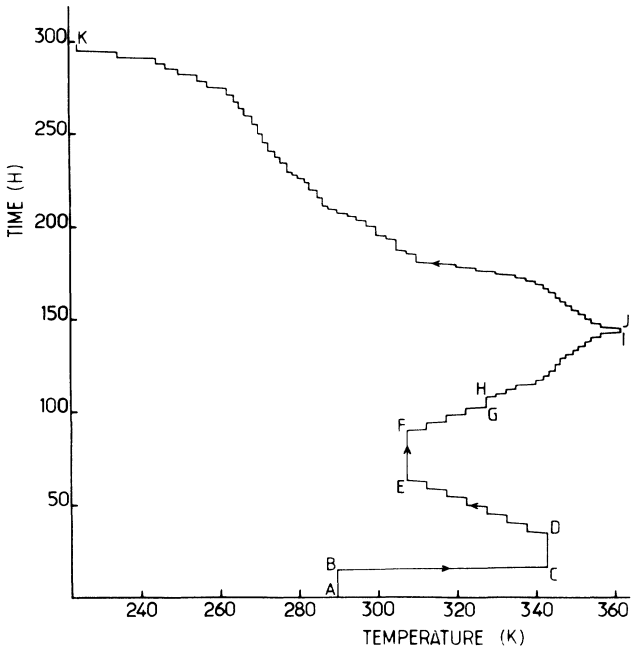

FIG. 7. Thermal history of ND_4DSeO_4 sample.

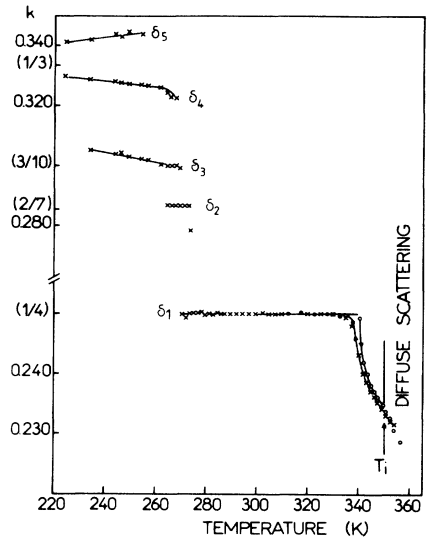

FIG. 8. Temperature dependence of the wave number $k(T)$ in ND_4DSeO_4, obtained during the cooling run (DE) (●), heating run (FI) (○), and cooling run (JK) (×), as shown in Fig. 4. Below 275 K, the results are obtained from the fit to the diffraction profiles (Fig. 10).

ment, except in the (002) zone where the (0 0 1.5198) and (0 0 2.4802) satellites are absent. As in the hydrogenated compound the satellite wave vector propagates along the c direction and is described by $\mathbf{k}_z = k\ (004\pi/c)$ with $k = 0.2401$ at $T = 342.7$ K. The transition at T_p (cf. Fig. 1) is not, as assumed up to now, a transition from the $P2_12_12_1$ phase to the paraelectric $B2$ one but to an incommensurate phase with a parent lattice of $B2$ symmetry.

2. *First cooling run and second heating run: stability and metastability of the lock-in $\frac{1}{4}$ and incommensurate phases*

In the subsequent first cooling run [path (DE), Fig. 7], the satellite wave number k is found to increase with decreasing temperature. Then at $T \sim 337$ K it locks in onto the rational value $k = \frac{1}{4}$ (cf. Fig. 8) ($2c$ superstructure). The parent lattice of this $\frac{1}{4}$ lock-in phase has the monoclinic $B2$ symmetry. The width of the satellite reflection is in the limit of the resolution, except in the vicinity of the lock-in phase transition, and no higher-order-satellite reflections could be detected even near the lock-in phase. During this cooling run, the satellite intensity regularly increases with decreasing temperature, but suddenly at $T = 307.1$ K an abrupt decrease of intensity is observed. This decrease is counterbalanced by the appearance and an increase of intensity of the (021) reflection (cf. Fig. 3), demonstrating an *oriented* growth of the $P2_12_12_1$ phase within the $2c$-superstructure phase ($k = \frac{1}{4}$). The two phases have interplanar distances which are slightly different. Measurements give, for the $2c$-superstructure phase, $d_{(\bar{1}10)} = 4.623$ Å and $d_{(001)} = 7.560$ Å. This should be compared with $d_{(010)} = 4.609$ Å and $d_{(001)} = 7.518$ Å for the $P2_12_12_1$ phase. A diminution of interplanar distances for the $P2_12_12_1$ phase of 0.30% and 0.56%, respectively, in perfect agreement with previous x-ray results[4] has been found. At this temperature $T = 307.1$ K, the kinetics has been studied along the (EF) path and the results of the intensity variation of the (021) Bragg reflection being a signal of $P2_12_12_1$ phase and $(\bar{2}\,2 \pm \frac{1}{2})$ satellites being a signal of the $2c$ superstructure, are illustrated in Figs. 9(a) and 9(b), respectively. The rate of evolution is maximum at the beginning and then decreases continuously with time. The characteristic time of variation of the intensity was too long and the saturation level was not reached after a time of 1600 min. Between F ($t = 1600$ min) and E ($t = 0$), we have observed a reduction of $\sim 55\%$ of the satellite intensity.

After investigation of the kinetics at $T = 307.1$ K, the crystal was reheated [path ($F \ldots I$), Fig. 7]. A comparison of the new data with those taken during the first cooling run revealed a reduction factor for satellite intensity which remains approximately constant ($\sim 55\%$) up to 327.4 K. At this temperature, the following effects appear during the path (GH) (Fig. 7): (i) the intensity of the (021) Bragg reflection quickly decreases with time and a reduction factor of 95% is reached after 3 h, and (ii) simultaneously a rapid decrease of the ($\bar{2}20$) and (002) Bragg intensities is observed during the first two hours. The saturation level is reached after 5 h. Comparing now these intensities with the intensities obtained at the same temperature during the cooling run reduction factors of $\sim 40\%$ and $\sim 25\%$ for the ($\bar{2}20$) and (002) Bragg reflection, respectively, are found. Finally, comparing at $T = 342.5$ K the present satellite intensity with that obtained during the first cooling run, we obtained a reduction factor of $\sim 45\%$.

The above observations allow us to draw the following conclusions.

(i) Below ~ 307 K, the phase of $2c$ superstructure

($k=\frac{1}{4}$) transforms into the stable $P2_12_12_1$ orthorhombic phase, the kinetics of transformation being very slow.

(ii) Keeping the crystal about one day at 307.1 K, part of the sample was transformed into the orthorhombic $P2_12_12_1$ phase. We estimate that from that $\sim 10\%$ conserved the crystallographic relationship as drawn in Fig. 3 while $\sim 45\%$ does not.

(iii) Reheating from 307.1 to 322 K did not change the amount of the $P2_12_12_1$ phase embedded into the $2c$ superstructure.

(iv) A recovery of $2c$-superstructure phase ($k=\frac{1}{4}$) is observed at 327.4 K but the sample is no longer a single crystal, since only 55% of specimen conserves the same initial orientational relationship.

After studying these nonequilibrium phenomena, the warming run was continued up to 361.5 K [path (*HI*), Fig. 7] and Fig. 8 shows the results. With increasing temperature, the lock-in phase ($k=\frac{1}{4}$) is found to be stable up to $T\sim 340.5$ K. Then, the wave vector decreases down to $k(T_i=350.5\text{ K})=0.2343$. Note the rapid decrease of k near the lock-in transition. An incommensurate phase exists in the narrow temperature interval (342.5–350.5 K). Above T_i, in the monoclinic phase of space group $B2$ the incommensurate phase is announced by remarkable critical diffuse scattering.

3. *Second cooling run: phase transitions between the lock-in phases $\frac{1}{4}$ and $\frac{1}{3}$*

To study further the phase diagram, a second cooling run down to $T=224$ K has been performed [path (*JK*), Fig. 7].

(a) Results above 275 K: lock-in phase $\frac{1}{4}$. Starting the measurements with the sample in the monoclinic $B2$

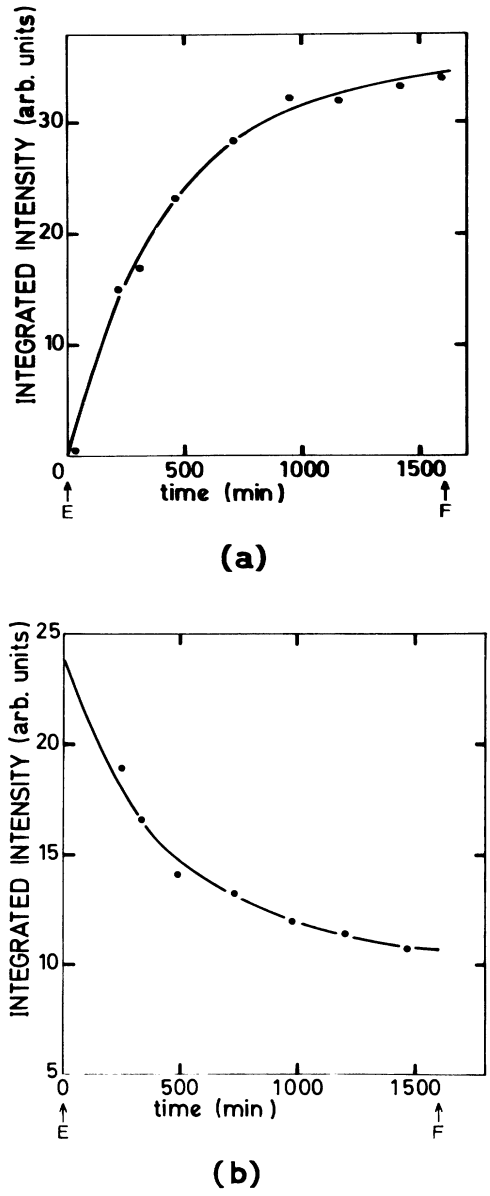

FIG. 9. (a) integrated intensity of the Bragg reflection (021) and (b) integrated intensity of the satellite reflection ($\bar{2}\,2\pm\frac{1}{2}$) as a function of time at $T=307.1$ K for ND_4DSeO_4.

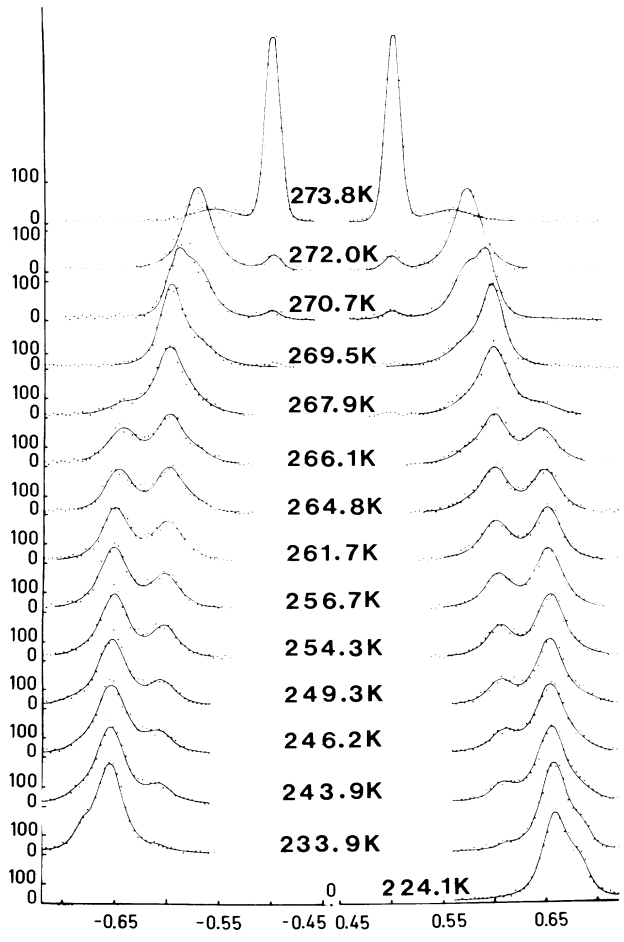

FIG. 10. Scans along the $[\bar{2}2\zeta]$ direction at different temperatures for ND_4DSeO_4. The lines represent computer fits based on a sum of two or three Lorentzian profiles centered in $\mathbf{k}_z^i$, and convoluted with the experimental resolution.

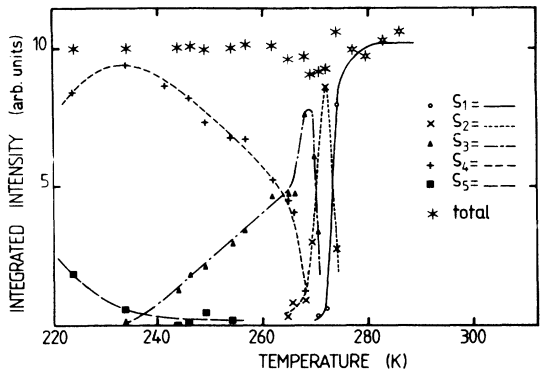

FIG. 11. Integrated intensity of the different satellite peaks as a function of temperature for ND_4DSeO_4. Results are obtained from the fit to the diffraction profiles (Fig. 10).

phase ($T > T_i = 350.5$ K) and decreasing the temperature, the incommensurate phase is found to be stable down to 337 K. Global hysteresis on the k wave number dependence is observed throughout the incommensurate phase. The lock-in phase of $2c$ superstructure ($k = \frac{1}{4}$) is observed in a large temperature interval (237, ~275 K) (cf. Fig. 8). In this phase, at $T = 309.5$ K, approximately the same temperature as in the first cooling run, a sudden decrease of the Bragg ($\bar{2}20$) and (002) and satellite intensities is observed, the reduction factor being about 15–20 %, but this time no intensity in the (021) point has been detected. We conclude that below a temperature $T_{gr} \sim 310$ K, the phase $P2_12_12_1$ develops within the modulated phase.

(b) Results below 275 K: observation of quasisteps.

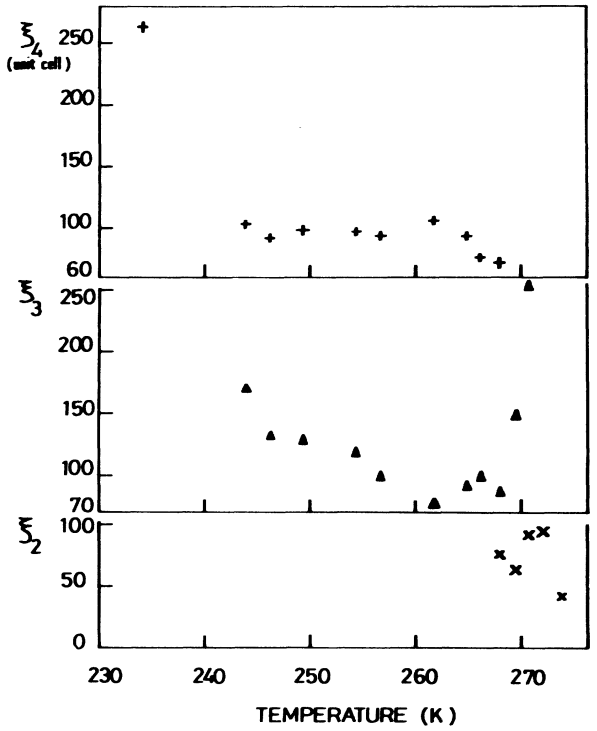

FIG. 12. Correlation lengths ξ_i, $i = 2,3,4$ in unit-cell units along the c direction as a function of temperature for ND_4DSeO_4. Results are obtained from the fit to the diffraction profiles (Fig. 10).

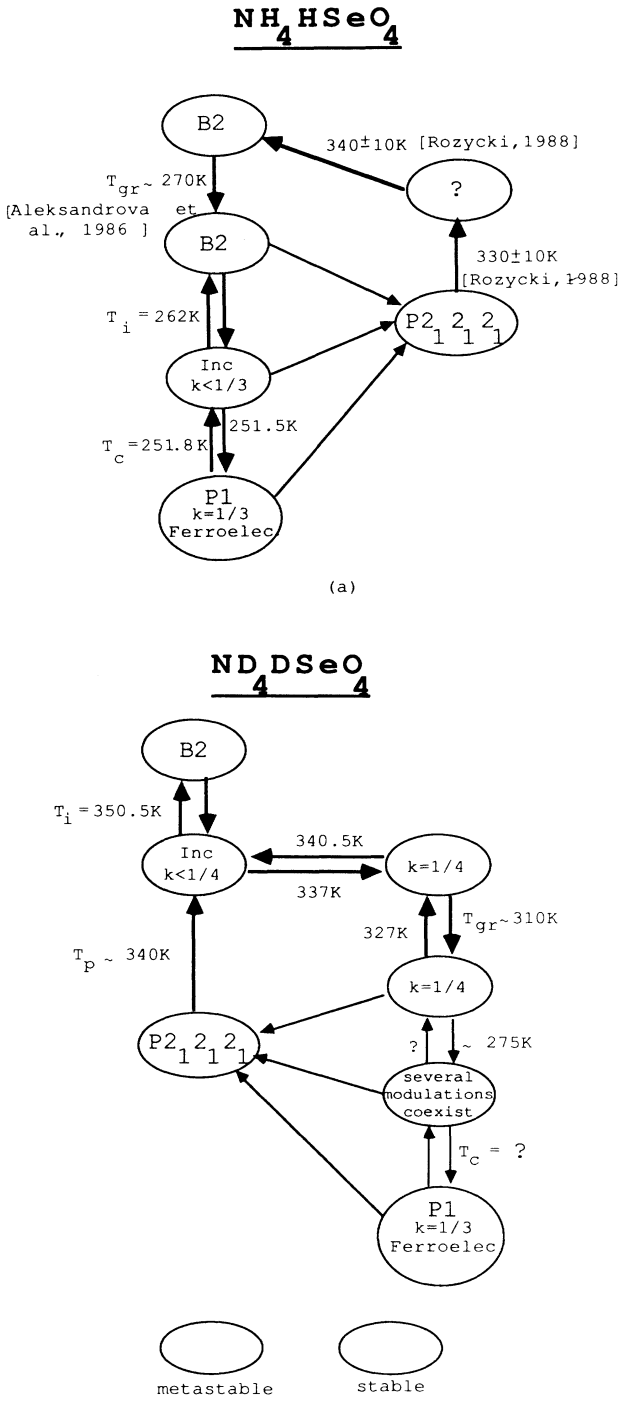

FIG. 13. Stable and metastable phase sequences in (a) NH_4HSeO_4 and (b) ND_4DSeO_4.

Below 275 K, scans along the $[\bar{2}2\zeta]$ direction revealed new interesting features (cf. Fig. 10). The satellites at $(\bar{2}\,2\pm0.5)$, corresponding to wave number $k=\frac{1}{4}$, disappear. When temperature further decreases, profiles composed of two or three peaks are observed. These peaks are centered in the vicinity of the $(\bar{2}\,2\sim\pm\frac{4}{7})$, $(\bar{2}\,2\sim\pm\frac{3}{5})$, and $(\bar{2}\,2\sim\pm\frac{2}{3})$ positions. The sample is in a state where several modulations of slightly different lengths coexist. The modulations propagate along the **c** direction and the modulation wave vectors can be written as $\mathbf{k}_z^i=\delta_i(0\,0\,4\pi/c)$ with $i=2,\ldots,5$. Figure 8 shows the variations of wave numbers $k(T)$ which consist of quasisteps situated approximately at $\delta_2\sim\frac{2}{7}$, $\delta_3\sim\frac{3}{10}$, $\delta_4\sim(\frac{1}{3})-\epsilon$, and $\delta_5\sim(\frac{1}{3})+\epsilon$. The peaks are broadened in the direction of the modulation. The experimental profiles (Fig. 10) can be described as a sum of two or three Lorentzians centered around $\mathbf{k}_z^i$ and convoluted with the experimental resolution. The variation of the integrated intensity in each modulation component is plotted as a function of temperature T in Fig. 11. Subtle intensity transfers are observed between the different peaks, but the total intensity remains constant. Below 275 K, a very small broadening of the (220) Bragg reflection in the **c** direction is observed. This effect is due to a very slight increase, with decreasing temperature, of the angle between the $[\bar{1}10]$ and [001] directions. Figure 12 reports the corresponding correlation length ξ_i for each satellite peak δ_i, $i=2,3,4$. In these calculations the broadening effect of Bragg reflections has been taken into consideration. The correlation lengths are of order of 100 unit cell units along the **c** direction. One notices that below 275 K the kinetics of transformation of the observed phases into the $P2_12_12_1$ orthorhombic one is very slow in comparison with the rate of our cooling run[12] and therefore this additional complication can be neglected.

We summarize the phase situation of NH_4HSeO_4 and ND_4DSeO_4 in Fig. 13. Comparing this figure with the phase diagram in Fig. 1, we see that the intermediate phase of the hydrogenated compound can be identified with the incommensurate phase while the deuterated crystal has in the range of the intermediate phase the incommensurate and lock-in $k=\frac{1}{4}$ phases.

IV. GROUP-THEORETICAL ANALYSIS OF INCOMMENSURATE PHASES

The reference structure is monoclinic base centered on the face (a,c) with the space group $B2$ [Fig. 2(a)]. The one-dimensional incommensurate modulation propagates along the **c** direction. Therefore the group-theoretical analysis of the incommensurate phases should be performed in terms of the irreducible representations of the star of $\mathbf{k}_z$ with the wave vector $\mathbf{k}_z=k(\mathbf{b}_2-\mathbf{b}_3)=k(0\,0\,4\pi/c)$ in the Kovalev notation.[13] There are two one-dimensional irreducible representations related with the star of $\mathbf{k}_z$, and both are complex. To make them physically irreducible, one should impose additionally the time reversal symmetry.[14] For that we enlarge the space group $B2$ by supplementing it with a time reversal symmetry element K. The corresponding physically irreducible representations $D^{(k,1)}$ and $D^{(k,2)}$ are two-dimensional (Table I). We denote their basic functions as $\psi_1(k),\psi_1^*(k)$ and $\psi_2(k),\psi_2^*(k)$, respectively. Using the standard projection operator technique and setting $\psi_i(k)=(\frac{1}{2})\eta_i(k)\exp[-i\epsilon_i(k)]$, where the amplitude $\eta_i(k)$ and the phase $\epsilon_i(k)$ are real, and $i=1,2$ denotes the $D^{(k,1)}$ and $D^{(k,2)}$ representations, the invariant of the pth order can be found:

$$I_p[\psi_i(k_1),\psi_i(k_2),\ldots\psi_i(k_p)]=(1/2^p)\eta_i(k_1)\eta_i(k_2)\cdots\eta_i(k_p)\cos[\varepsilon_i(k_1)+\varepsilon_i(k_2)+\cdots+\varepsilon_i(k_p)]\times\delta[k_1+k_2+\cdots+k_p-m(4\pi/c)]\,, \tag{1}$$

where m is an integer. Only even $p=2,4,6,\ldots$ invariants exist for $D^{(k,2)}$ representation while all $p=2,3,4,\ldots$ exist for $D^{(k,1)}$.

The incommensurate phases in NH_4HSeO_4 and ND_4DSeO_4 are described by the $D^{(k,2)}$ representation. This representation has been selected because of the following arguments. The low-temperature triclinic phase $P1$ is ferroelectric with the spontaneous polarization being parallel to the **b** axis. It is a lock-in phase $\frac{1}{3}$. Only the $D^{(k,2)}$ representation can generate the lock-in phase $\frac{1}{3}$ being ferroelectric. The representation $D^{(k,1)}$ can lead to even stronger lock-in phase $\frac{1}{3}$, but not ferroelectric.

TABLE I. The physically irreducible representations of the star $\mathbf{k}_z=k(0\,0\,4\pi/c)$ of the space groups $B2+K\,B2$. The E and K are the identity and time reversal symmetry elements, respectively. The $\{h_i|\mathbf{t}_n\}$ is the symmetry element in Kovalev's (Ref. 13) notation, and $\mathbf{t}_n=n_x\mathbf{a}+n_y\mathbf{b}+n_z\mathbf{c}$ and $\alpha=\exp(2\pi\mathbf{k}_z\cdot\mathbf{t}_n)$.

	$\{h_1\|t_n\|E\}$	$\{h_1\|t_n\|K\}$	$\{h_4\|t_n\|E\}$	$\{h_4\|t_n\|K\}$
$D^{(k,1)}$	$\begin{bmatrix}\alpha^* & 0\\ 0 & \alpha\end{bmatrix}$	$\begin{bmatrix}0 & \alpha\\ \alpha^* & 0\end{bmatrix}$	$\begin{bmatrix}\alpha^* & 0\\ 0 & \alpha\end{bmatrix}$	$\begin{bmatrix}0 & \alpha\\ \alpha^* & 0\end{bmatrix}$
$D^{(k,2)}$	$\begin{bmatrix}\alpha & 0\\ 0 & \alpha\end{bmatrix}$	$\begin{bmatrix}0 & \alpha\\ \alpha^* & 0\end{bmatrix}$	$\begin{bmatrix}-\alpha^* & 0\\ 0 & -\alpha\end{bmatrix}$	$\begin{bmatrix}0 & -\alpha\\ -\alpha^* & 0\end{bmatrix}$

Thus the free energy consists of second- and fourth-order terms only:

$$F=(\tfrac{1}{4})\sum_{k_1,k_2}\omega(k_1,k_2)\eta(k_1)\eta(k_2)\cos[\varepsilon(k_1)+\varepsilon(k_2)]\delta(k_1+k_2-m(4\pi/c))$$
$$+(\tfrac{1}{16})\sum_{k_1,k_2,k_3,k_4}C(k_1,k_2,k_3,k_4)\eta(k_1)\eta(k_2)\eta(k_3)\eta(k_4)$$
$$\times\cos[\varepsilon(k_1)+\varepsilon(k_2)+\varepsilon(k_3)+\varepsilon(k_4)]\delta(k_1+k_2+k_3+k_4-m(4\pi/c))\ , \tag{2}$$

where the index $i=2$ has been suppressed. This form of the free energy has allowed us to analyze[15] the possible lock-in phases. In particular, one finds the following properties.

(i) The lock-in phase $\frac{1}{4}$. It arises owing to the lock-in term of fourth order between the first harmonics $(\frac{1}{4},\frac{1}{4},\frac{1}{4},\frac{1}{4})$. It is not ferroelectric and four domains of it exist.

(ii) The lock-in phase $\frac{1}{3}$. This phase is locked by the term $(\frac{1}{3},\frac{1}{3},\frac{1}{3},0)$ relating the first- and zeroth-order harmonics. The last one represents the strain yz,xz and the spontaneous polarization. It is ferroelectric and six domains exist.

(iii) The lock-in phase $\frac{2}{7}$. The lock-in term relates the first-, third-, and zeroth-order harmonics $(\frac{2}{7},\frac{2}{7},\frac{6}{7},0)$; therefore, the phase is ferroelectric. The number of domains is 14.

(iv) The lock-in phase $\frac{3}{10}$. This phase arises from the coupling between the first- and third-order harmonics $(\frac{3}{10},\frac{9}{10},\frac{9}{10},\frac{9}{10})$. The phase is not ferroelectric and 10 domains exist.

All above-listed lock-in phases are described by the space group $P1$.

The assignment of the observed steps, Fig. 8, to the commensurate lock-in phases is tentative, but there are arguments which introduce doubts in these procedures. The lock-in phases $\frac{2}{7}$ and $\frac{3}{10}$ depend on the amplitude of the third-order harmonics, but for these phases no third-order satellites were detected. All the quasisteps coexist in the range of temperature almost as wide as the existence of each phase, which is unusual for the devil's-staircase behavior. Then, some doubts can be raised from the fact that such well-defined steps at commensurate values already appear with the system still not being in an equilibrium state.

V. FINAL REMARKS

The existence of the incommensurate modulation and the low-temperature lock-in phase $k=\frac{1}{3}$ in hydrogenated NH_4HSeO_4 is similar to that in other incommensurate materials. It is, however, remarkable that the incommensurate phase is already a long-living metastable state.

The situation is even more complicated in deuterated ND_4DSeO_4. On cooling, the incommensurate phase is locked at the wave number $k=\frac{1}{4}$ and subsequently a coexistence of several intermediate modulations is observed. These modulations precede the appearance of the ferroelectric lock-in phase $k=\frac{1}{3}$.

One possibility is that these modulations are not the true equilibrium lock-in phases but intermediate stages which arise in the process of the first-order phase transition from the $k=\frac{1}{4}$ to the $k=\frac{1}{3}$ lock-in phase. In such a case, the equilibrium devil's staircase of ND_4DSeO_4 will contain two lock-in steps: one below 275 K at $k=\frac{1}{3}$, second above that temperature at $k=\frac{1}{4}$. This statement is supported by the following arguments: The quasisteps occur simultaneously in some range of temperature and their wave numbers are not exactly locked in at the commensurate values. The group-theoretical consideration says that the equilibrium lock-in phases $k=\frac{2}{7}$ and $\frac{3}{10}$ should be accompanied by higher-order harmonics, but these harmonics have not been observed. Finally, the kinetics of the phase transitions from the lock-in phase $\frac{1}{4}$ to $\frac{1}{3}$ is, perhaps, remarkably hindered by insertion of the $P2_12_12_1$ grains and incomplete deuteration of the crystal.

The mechanism of the phase transition between two strong lock-in phases is not yet fully understood. The conventional stripple mechanism[16–19] with the discommensuration planes cannot be applied here. Instead, one should expect that the thermal fluctuations will locally nucleate a nucleus of the $\frac{1}{3}$ modulation. Along the direction of the modulation such a nucleus will match to the $k=\frac{1}{4}$ modulation but it must make mismatch fronts in the lateral directions. Since for the nucleation process thermal fluctuations are sufficient, a macroscopic number of such nuclei can appear simultaneously. They grow and lead to a nonequilibrium "microstructure" of the lock-in phase $k=\frac{1}{3}$ with a remarkable number of "stacking faults" in the form of thin insertions of the $k=\frac{1}{4}$ modulation. At different stages of the transition, this microstructure shows up in the diffraction experiment as characterized by rather simple wave numbers. Although the microstructure is unstable a considerable effort is needed to remove it. The reason is that a removal of the stacking faults will involve a reconstruction of vast regions of the crystal.

Another possibility is that between the two strong lock-in phases $k=\frac{1}{4}$ and $k=\frac{1}{3}$ a narrow insertion of either incommensurate or commensurate phase is present in the equilibrium devil's staircase of the ND_4DSeO_4. The new experimental data[20] have shown that the quasisteps in the cooling and heating runs occur in a partly overlapping region of temperatures, and such a behavior is in contradiction with the expectations for the phase transition between two strong lock-in phases. In

the last case the quasisteps of cooling and heating runs should occur in separated temperature intervals.

ACKNOWLEDGMENTS

The authors would like to thank J. M. Godard for growing the NH_4HSeO_4 and ND_4DSeO_4 crystals, N. Lenain for delicate preparation of samples, and P. Boutrouille for his efficient technical assistance during the course of the measurements. The Laboratoire de Physique des Solides is "Associé au Centre National de la Recherche Scientifique." The Laboratoire Léon Brillouin is "Laboratoire Commun Commissariat à l'Energie Atomique–Centre National de la Recherche Scientifique." The Laboratoire de Dynamique des Cristaux Moléculaires is "Unité Associé au Centre National de la Recherche Scientifique No. 801."

---

*Permanent address: Institute of Nuclear Physics, ul. Radzikowskiego, 152, PL-31-342 Cracow, Poland.

†Permanent address: Laboratoire de Dynamique des Cristaux Moléculaires Université de Lille I, 59655 Villeneuve d'Ascq Cédex, France.

[1]I. P. Aleksandrova, Yu. N. Moskvich, O. V. Rozanov, A. F. Sadreev, I. V. Seryukova, and A. A. Sukhovsky, Ferroelectrics **67**, 63 (1986), and references therein.

[2]K. S. Aleksandrov, A. I. Kruglik, S. V. Misyul', and M. A. Simonov, Kristallografiya **25**, 1142 (1980) [Sov. Phys.—Crystallogr. **25**, 654 (1980)].

[3]A. I. Kruglik, S. V. Misyul', and K. S. Aleksandrov, Dokl. Akad. Nauk SSSR **25**, 344 (1980) [Sov. Phys.—Dokl. **25**, 871 (1980)].

[4]A. Rozycki, F. Dénoyer, and A. Novak, J. Phys. (Paris) **48**, 1553 (1987).

[5]Z. Czapla, O. Czupinski, and L. Sobczyk, Solid State Commun. **40**, 929 (1981).

[6]A. Waskowska and Z. Czapla, Acta Crystallogr., Sec. B **38**, 2017 (1982).

[7]A. Rozycki, thesis, University of Paris, Paris, France, 1988.

[8]I. P. Aleksandrova, Yu. N. Moskvich, O. V. Rozanov, A. F. Sadreev, I. V. Seryukova, and A. A. Sukhovsky, Jpn. J. Appl. Phys. **24**, 856 (1985).

[9]Z. Czapla, O. Czupinski, and L. Sobczyk, Solid State Commun. **51**, 309 (1984).

[10]A. A. Sukhovsky, Yu. N. Moskvich, O. V. Rozanov, and I. P. Aleksandrova, Fiz. Tverd. Tela (Leningrad) **28**, 3368 (1986) [Sov. Phys.—Solid State **28**, 1896 (1986)].

[11]M. Descamps and C. Caucheteux, J. Phys. C **20**, 5073 (1987).

[12]P. Colomban, A. Rozycki, and A. Novak, Solid State Commun. (to be published).

[13]O. V. Kovalev, *Irreducible Representations of the Space Groups* (Gordon and Breach, New York, 1965).

[14]J. L. Birman, *Theory of Crystal Space Groups and Infra-Red and Raman Processes of Insulating Crystals,* Vol. 25/2b of *Handbuch der Physik* (Springer-Verlag, Berlin, 1974).

[15]K. Parlinski and F. Dénoyer, J. Phys. C **18**, 293 (1985).

[16]V. Janovec, Phys. Lett. **99A**, 384 (1983).

[17]K. K. Funk, S. McKernan, J. W. Steeds, and J. A. Wilson, J. Phys. C **14**, 5417 (1981).

[18]K. Parlinski and F. Dénoyer (unpublished).

[19]K. Parlinski, Phys. Rev. B **35**, 8680 (1987).

[20]F. Dénoyer, A. Rozycki, K. Parlinski, and M. More, Phase Transition (to be published).